Marine Chemistry 186 (2016) 58–71

Contents lists available at ScienceDirect

Marine Chemistry

journal homepage: www.elsevier.com/locate/marchem

Loadings of dissolved organic matter and nutrients from the Neva River into the Gulf of Finland – Biogeochemical composition and spatial distribution within the salinity gradient

Pasi Ylöstalo [a,*], Jukka Seppälä [a], Seppo Kaitala [a], Petri Maunula [a], Stefan Simis [a,b]

[a] Marine Research Centre, Finnish Environment Institute, P.O. Box 140, FIN-00251 Helsinki, Finland
[b] Plymouth Marine Laboratory, Prospect Place, The Hoe, PL1 3DH Plymouth, United Kingdom

ARTICLE INFO

Article history:
Received 2 November 2015
Received in revised form 30 June 2016
Accepted 25 July 2016
Available online 26 July 2016

Keywords:
Baltic Sea
River Neva
Estuaries
Riverine loading
Absorption
Chromophoric dissolved organic matter
Dissolved organic carbon
Carbon budgets
Dissolved organic nitrogen

ABSTRACT

We studied the loadings of dissolved organic matter (DOM) and nutrients from the Neva River into the Eastern Gulf of Finland, as well as their distribution within the salinity gradient. Concentrations of dissolved organic carbon (DOC) ranged from 390 to 840 μM, and were related to absorption of colored DOM (CDOM) at 350 nm, $a_{CDOM}(350)$, ranging from 2.70 to 17.8 m^{-1}. With increasing salinity both DOC and a_{CDOM} decreased, whereas the slope of a_{CDOM} spectra, $S_{CDOM}(300–700)$, ranging from 14.3 to 21.2 μm^{-1}, increased with salinity.

Deviations of these properties from conservative mixing models were occasionally observed within the salinity range of approximately 1–4, corresponding to the region between 27 and 29°E. These patterns are suggested to mostly reflect seasonal changes in properties of river end-member and hydrodynamics of the estuary, rather than non-conservative processes. On the other hand, observed nonlinear relationships observed between $a_{CDOM}{}^{*}(350)$ and $S_{CDOM}(275–295)$ emphasized the importance of photochemistry among various transformation processes of DOM.

Dissolved inorganic nitrogen was effectively transformed in the estuary into particulate organic nitrogen (PON) and dissolved organic nitrogen (DON), of which DON was mostly exported from the estuary, enhancing productivity in nitrogen limited parts of the Gulf of Finland. DON concentrations ranged from 12.4 to 23.5 μM and its estuarine dynamics were clearly uncoupled from DOC. In contrast to DOC, estuarine DON dynamics suggest that its production exceeds losses in the estuary.

Total nitrogen (TN) and phosphorus (TP) loadings from the Neva River and St. Petersburg were estimated as 73.5 Gg N yr^{-1} and 4.2 Gg P yr^{-1}, respectively. Approximately 59% of TN and 53% of TP loads were in organic forms. DOC and DON loadings were estimated as 741.4 Gg C yr^{-1} and 19.0 Gg N yr^{-1}, respectively. Our estimate for DOC loading was evaluated against a previously published carbon budget of the Baltic Sea. According to the updated model, the Baltic Sea could be identified as a weak source of carbon into the atmosphere.

1. Introduction

Eutrophication is recognized as the major environmental issue affecting the Baltic Sea, particularly in coastal regions (Elmgren, 2001). Eutrophication causes nuisance phytoplankton blooms and increased oxygen consumption leading to occasional loss of benthic flora and fauna, and release of nutrients from anoxic sediments (HELCOM, 2009). The Baltic Sea has a large catchment (1.7×10^6 km^2, approximately 4.5 times the surface area of the sea) which combined with a long renewal time (~25–35 years) and limited exchange with the North Sea makes it highly vulnerable to nutrient loadings from its catchment. The Helsinki Commission (HELCOM, 2012) attributes 75% of nitrogen and >95% of phosphorus loads into the Baltic Sea to waterborne inputs, i.e. direct discharges or via rivers. Riverine nitrogen and phosphorus loads, of which approximately only half is in inorganic form, are dominated by few large rivers: Neva, Vistula, Daugava, Oder, and Nemunas, contributing approximately half of all riverine loadings into the Baltic Sea (Stålnacke et al., 1999; HELCOM, 2012).

Riverine loadings of dissolved nutrients have been studied extensively while comparatively little is known about the quality, quantity, and effects of dissolved organic matter (DOM) on receiving waters (Mattsson et al., 2005). Allochthonous DOM has long been regarded as mostly refractory and biologically unavailable (e.g. Bronk et al., 2007). The present consensus is that microbial mineralization and photodegradation of DOM release inorganic carbon, organic molecules of low molecular-weight, and phosphorus- and nitrogen-rich compounds that fuel growth of aquatic micro-organisms, especially when inorganic nutrients are depleted (Vähätalo and Zepp, 2005). The colored

* Corresponding author: Finnish Environment Institute (SYKE), Marine Research Centre, P.O. Box 140, FIN-00251 Helsinki, Finland.
E-mail address: pasi.ylostalo@environment.fi (P. Ylöstalo).

http://dx.doi.org/10.1016/j.marchem.2016.07.004
0304-4203/

fraction of DOM absorbs light, especially at the UV and blue range of the spectrum, affecting the quality and quantity of light penetrating into the water column, and thus primary production, temperature stratification, as well as UV exposure of biota (Häder et al., 2007; Urtizberea et al., 2013; Thrane et al., 2014). Dissolved organic substances are also known to affect solubility, mobility and bioavailability of certain metals and organic chemicals, and thereby their toxicity to biota (Kördel et al., 1997; Akkanen et al., 2012).

Oceans are recognized as an important carbon sink in the global carbon cycle, regulating concentrations of atmospheric CO_2 (Carlson and Hansell, 2015). The Baltic Sea has both been identified as a sink incorporating 2.3–4.3 g C m^{-2} yr^{-1} into the sea (Thomas et al., 2010; Gustafsson et al., 2014) as well as a source releasing 2.7 g C m^{-2} yr^{-1} into the atmosphere (Kuliński and Pempkowiak, 2011). The range and associated confidence limits of these estimates indicates that both the magnitude of terrestrial carbon load and key processes of the aquatic carbon cycle are still poorly known. Estimates of riverine carbon load into the Baltic Sea range from 10.3 to 14.2 Tg C yr^{-1} of which the organic fraction constitutes 20 to 38% (Thomas et al., 2010; Kuliński and Pempkowiak, 2011; Gustafsson et al., 2014). Given their importance, accurate quantification of these riverine fluxes is prerequisite to model the carbon balance of the Baltic Sea, and to determine its role as a sink or a source of atmospheric carbon (Thomas et al., 2010). At present, knowledge of individual river fluxes is however severely limited, even with regard to some of the largest contributing rivers, such as the Neva River (Gustafsson et al., 2014).

Transformation of DOM over salinity gradients of estuaries and coastal waters is commonly observed, although the dynamics of the underlying physical and biogeochemical processes are relatively poorly understood. Studies of the chemical quality of DOM are increasingly based on the optical properties of its chromophoric components (CDOM), particularly the mass-specific absorption (a_{CDOM}^*, m^{-2} (mol DOC)$^{-1}$) and the slope of the absorption coefficient in the ultraviolet (UV) to visible domain (S_{CDOM}, μm^{-1}), which allow their use as proxies of molecular weight and C/N ratio of DOM (Helms et al., 2008; Fichot and Benner, 2012). Optical properties of DOM are also widely utilized for estimating DOC concentrations by applying ocean color data and measurements made with either fluorescence or absorption sensors to study the spatiotemporal distribution of DOC. Such estimates are based on the assumption of a constant relationship between optical properties of DOM and DOC, which may vary regionally and seasonally. The DOM pool consists of both colored and uncolored compounds mixed in varying proportions. Color and chemical composition are further affected by the origin of the DOM, and by subsequent transformation processes (Stedmon and Nelson, 2015).

Variations in the quality and quantity of DOM in coastal systems are related to mixing dynamics (Stedmon et al., 2010; Osburn and Stedmon, 2011), and to local loss and production processes: microbial and photo-induced degradation (Helms et al., 2008; Fichot and Benner, 2012), salinity-induced flocculation (Asmala et al., 2014), and autochthonous production of DOM (Kowalczuk et al., 2006; Fichot and Benner, 2012). Linear relationships between DOM or a_{CDOM} and salinity are generally taken as evidence of an allochthonous DOM origin and conservative mixing into the sea, whereas deviations from linearity are related to non-conservative processes, or more complex mixing of water masses (e.g. Abril et al., 2002; Stedmon et al., 2010; Markager et al., 2011).

Given the important influence of catchment processes on the ecological state and carbon balance of the Baltic Sea and particularly on the most nutrient-enriched sub-basins, detailed information on riverine nutrient and carbon loads is needed. The aim of this study is to estimate loadings of dissolved organic carbon (DOC) and nitrogen (DON) from the Neva River, the largest river draining into the Baltic Sea. Based on combined analysis of optical and biogeochemical observations and mixing models, this study aims to contribute a better understanding of the spatiotemporal behavior of these organic constituents within and beyond the river estuary. While focus of this work is on DOM, concentration and loading estimates of other major nutrients are provided to allow comparison of present results with former studies, and because the dynamics of nutrient and DOM pools are, at least at times, linked.

2. Methods

2.1. Study area

The studied sea area (Fig. 1) was divided into the Eastern Gulf of Finland (EGoF) and the Neva Estuary (NE), of which the latter one was

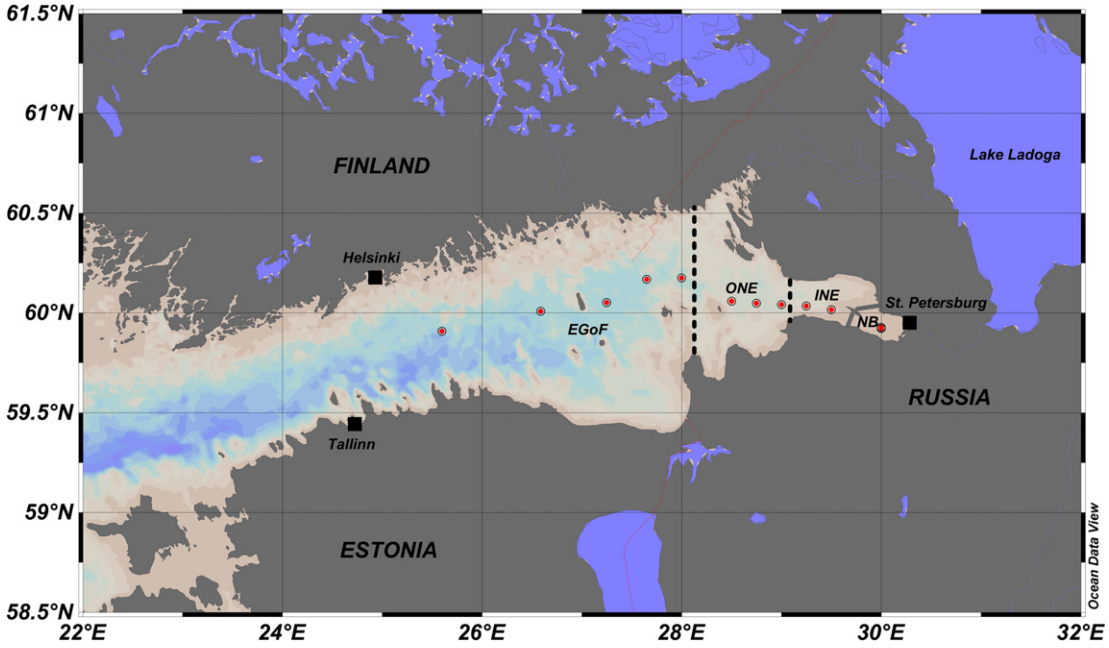

Fig. 1. Map of the Gulf of Finland, divided into sub-regions: the eastern Gulf of Finland (EGoF), the Outer Neva Estuary (ONE), the Inner Neva Estuary (INE), and the Neva Bay (NB). Grey drawn lines around NB indicate the dam separating the Neva Bay from the rest of the estuary. Red symbols represent sampling stations along the route of MS Silja Opera. (For interpretation of the references to color in this figure legend, the reader is referred to the web version of this article.)

further divided into three sub-regions: the Outer Neva Estuary (ONE), the Inner Neva Estuary (INE), and the Neva Bay (NB), following the definition of Pitkänen and Tamminen (1995). The Neva Bay is separated from the rest of the estuary by a flood-protection dam (indicated in Fig. 1), with only narrow sluices and water ways.

The Neva River (mean annual flow = 2500 $m^3 s^{-1}$) is the largest river draining to the Baltic Sea, corresponding to approximately 70% and 16% of the total runoff into the Gulf of Finland and the Baltic Sea, respectively (Bergström and Carlsson, 1994). Its catchment area (281,000 km^2) consist of 55% forest, 13% peat land, and 17% lakes (HELCOM, 1993). The river itself is a 74 km long channel, receiving most of its water through Lake Ladoga (17,891 km^2; Bergström and Carlsson, 1994; Drabkova et al., 1996) and therefore its dynamics reflect the hydrological regime of this lake. Precipitation into the Ladoga catchment is generally high from July to January (Golitsyn et al., 2002). During winter most of the precipitation falls as snow, which is primarily stored until spring melt. Consequently, inflow into the lake is most significant between April and June, whereas the outflow remains relatively constant during the period from March to November (Golitsyn et al., 2002). There are three other large lakes in the catchment (HELCOM, 1993; Drabkova et al., 1996): Lake Onega (9700 km^2), Lake Saimaa (4400 km^2), and Lake Ilmen (982 km^2). These lakes dampen seasonal fluctuations (Bergström and Carlsson, 1994) and retain and transform a large fraction of substances originating from the catchment (Drabkova et al., 1996; Kuuppo et al., 2006; Kondratyev, 2011). With regard to nitrogen, it has been estimated that 74% of the total load from the Neva catchment is retained within its lakes and streams (Stålnacke et al., 2015). Before entering the Gulf of Finland the Neva River flows through the city of St. Petersburg (5 million inhabitants), whose municipal loads contribute significantly to nitrogen (~25%) and phosphorus (~60%) loadings into the Gulf of Finland (Kiirikki et al., 2003; Kondratyev and Trumbull, 2012).

The Gulf of Finland is one of the most eutrophic sub-basins of the Baltic Sea (Kondratyev, 2011). The basin has a large catchment area (421,000 km^2) compared to its volume (1100 km^3) and area (30,000 km^2, Pitkänen et al., 2008). High runoff of the Neva River relative to the volume of the receiving basin creates strong horizontal gradients in salinity (increasing westward), as well as in dissolved organic matter and nutrients (decreasing westward). These gradients are further reflected in distributions of phytoplankton biomass and activity (Pitkänen and Tamminen, 1995; Andrejev et al., 2004; Pitkänen et al., 2008). Freshwater flow also affects vertical stratification of the water column (Andrejev et al., 2004; Jönsson et al., 2011). Water exchange between the Gulf of Finland and the Northern Baltic Proper is known to be very intensive. Andrejev et al. (2004) estimated a renewal time of water masses of the entire Gulf of Finland around 1–2 years, and determined that the water-age distribution in the gulf is spatially non-homogeneous with the highest age (approximately 2 years in the near surface layer between 2.5 and 7.5 m) in the south-eastern part of the Gulf (southeast from Moshnyi Island).

2.2. Sample collection and preparation

Samples were collected from MS Silja Opera, a ship-of-opportunity in the Alg@line network, operated between St. Petersburg and Helsinki. The study period, from mid-April till mid-December 2005 covered most of the ice free season (mid-April 2005 to late-January 2006). Temperature and salinity were recorded at 20-s intervals along the ship route with a thermo-salinograph (Aanderaa) placed in a flow-through system of sea water with the inlet at approx. 4 m depth. Discrete water samples were automatically stored at predefined locations using an Isco 3700 R refrigerated (+4 °C) sampler connected to the same system. Collected samples were stored in the sampler for 2–14 h depending on sampling time. Details of this monitoring system can be found in Leppänen and Rantajärvi (1995); Leppänen et al. (1995) and Seppälä et al. (2007). Samples were transferred to the laboratory for further processing upon arrival of the ship in Helsinki. Subsamples for measurements of light absorption of CDOM and concentrations of DOC and total dissolved nitrogen (TDN) were filtered through 0.2-μm syringe filters (Minisart, Sartorius), first washed with Milli-Q water and the water sample, into acid-washed and combusted glass vials sealed with Teflon-lined caps. CDOM samples were then stored without preservation agents at +4 °C in darkness until measurement within <1 week. Samples for DOC and TDN analysis were preserved with 2 M HCl and stored as above until analysis within <6 months. These storage times have been observed not to cause significant effects on either CDOM absorption (Stedmon et al., 2000) or DOC and DON concentrations (Lignell et al., 2008).

2.3. Optical and chemical analysis

CDOM absorption was measured with a spectrophotometer (Shimadzu UV-2101PC) with samples and an ultrapure water reference at room temperature. Absorbance was recorded over the 200 to 800 nm wavelength range and converted to absorption coefficients following:

$$a_{CDOM}(\lambda) = A_{CDOM}(\lambda) \times \ln(10) \times l^{-1} \quad (1)$$

where $A_{CDOM}(\lambda)$ is absorbance at wavelength λ and l is the path length of the quartz cuvette (0.1 m). In further analyses, only the 250–800 nm range is used due to potential influence of dissolved inorganic compounds (e.g. nitrate, nitrite, bisulfide and bromide) at shorter wavelengths (Johnson and Coletti, 2002). Absorption coefficients of CDOM are reported at 350 nm and 442 nm, the latter band for reference in long-term remote sensing studies using ocean color satellites.

The slope coefficient (S_{CDOM}, μm^{-1}) describing the exponential decrease of absorption with wavelength was determined by non-linear fitting of an exponential equation with offset correction (Warnock et al., 1999; Stedmon et al., 2000), using the *lsqcurvefit* routine in MATLAB:

$$a_{CDOM}(\lambda) = a_{CDOM}(350) \exp^{-S_{CDOM}(\lambda-350)} + K, \quad (2)$$

where $a_{CDOM}(350)$ is absorption at reference wavelength 350 nm, and *K* is an offset allowing for small baseline shifts or residual scattering. To enable comparison of our results to previous studies, and to ensure their applicability for various applications, $S_{CDOM}(\lambda_1 - \lambda_2)$ was determined over two wavelength ranges: 300–700 and 400–700 nm, the latter reported for its relevance in remote sensing applications.

In addition to the data collected for this study, spectral absorption data from phototransformation experiments carried out during 2006–2007 (Aarnos et al., 2012) were reprocessed, and results are included here where applicable. For this additional data set (based on samples from the Neva Bay, Central Gulf of Finland, the Northern Baltic Proper, Eastern Gotland Basin, and Arkona Basin) slopes were also calculated for the wavelength range 275–295 nm, according to Helms et al. (2008).

DOC and TDN concentrations were measured by high-temperature catalytic oxidation and non-dispersive infrared (NDIR) detection using a TOC analyzer (Shimadzu TOC-VCPH) equipped with chemiluminescence detector (Shimadzu TNM-1), for a subset of samples. Three replicates for each sample were divided over separate runs and subsequently averaged. Each run was calibrated with potassium hydrogen phthalate and ammonium sulfate. The DOC-specific CDOM absorption coefficient ($a_{CDOM}^*(350)$) was obtained by dividing $a_{CDOM}(\lambda)$ over the DOC concentration. The DON concentration was calculated by subtracting measured concentrations of dissolved inorganic nitrogen (DIN) fractions from TDN.

Concentrations of inorganic nutrients were measured using standard methods: nitrite (NO_2), nitrate (NO_3), and phosphate (PO_4) using flow injection analysis with colorimetric detection (Lachat Quikchem FIA + 8000 series), and ammonium (NH_4) manually with a spectrophotometer (Hanssen and Koroleff, 1999; Solórzano, 1969). Total nitrogen (TN) and phosphorus (TP) were measured as NO_3 and PO_4 after wet

oxidation with alkaline peroxodisulfate. Total organic nitrogen (TON) and phosphorus (TOP) were calculated by subtracting DIN and PO_4 from TN and TP, and particulate organic nitrogen (PON) by subtracting DON from TON, respectively.

The concentration of Chlorophyll-*a* (Chl *a*) was determined from subsamples concentrated onto Whatman GF/F filters and extracted with 96% ethanol for 24 h at room temperature in darkness. Pigment extracts were quantified with a spectrofluorometer calibrated with pure Chl *a* (Sigma), using 430 nm excitation and 668 nm emission wavebands with slit widths of 10 nm.

Figures representing the spatial and seasonal distribution of several in-water constituents were produced with Ocean Data View (Schlitzer, 2014) using its DIVA gridding option. Effects of various production and loss processes of DOM, and conservative mixing on observed DOM distribution was evaluated by comparing observed and modelled relationships of a_{CDOM}, S_{CDOM}, DOC and DON against salinity as a conservative tracer (cf. Stedmon and Markager, 2003). Due to seasonal variability of the concentrations and optical properties of particularly the freshwater end-member, mixing models with a river and sea end-member were calculated separately for each transect. The westernmost sample, having near-zero salinity, was used to represent the river end-member, and the westernmost sample (usually showing highest salinity) was used to represent the sea end-member.

Annual loadings of DOC and nutrient fractions were calculated based on available data as sums of discharge-weighted monthly average concentrations, multiplied by the annual discharge (Quilbé et al., 2006, Supplement 1). Flow rates for the studied period were based on measurements at Novosaratovka, located 27 km upstream from the mouth of Neva River (Sergey Kondratyev, pers. comm.). Loading estimates into the Gulf of Finland are based on concentrations measured in the Neva Bay, and these should therefore not be considered as loadings originating only from the Neva River, but as combined loadings from the Neva River and various point and diffusive sources of St. Petersburg. Effects of gaps in our monthly concentration data on loading estimates of both total and dissolved inorganic nutrients were evaluated by recalculating loadings, after data gaps were filled by: (1) adopting mid-April concentrations for missing data in January–March; (2) interpolating adjacent values to fill a gap in July; (3) predicting TP from the observed relationship between TP and TN for December. Support for the above approach is obtained from a previous study, describing seasonal variation of nutrient concentrations in the Neva River (Kuuppo et al., 2006).

3. Results

3.1. River discharge

During the studied period, monthly flow rates of the Neva River varied between 1810 and 3650 $m^3\ s^{-1}$, corresponding to annual runoff of approximately 91 km^3, the highest measured in the period 2000–2010 (Fig. 2). Despite higher peak discharge periods, seasonal flow of the river followed its long-term average pattern. During winter months, flow rates were low (1800 to 2290 $m^3\ s^{-1}$). Following snow melt, flow rates increased in April reaching a maximum of 3650 $m^3\ s^{-1}$ in June. After this maximum, flow rates decreased steadily towards winter.

3.2. Temperature, salinity and chlorophyll-a

Water temperatures at the surface layer varied seasonally from 0.1 °C in late April to 21.8 °C in late July (Fig. 3a). The semi-enclosed NB can be considered freshwater while salinity increased to 5.9 in the EGoF (Fig. 3b). In open sea areas, salinity followed a seasonal trend with higher salinities observed during the spring and autumn compared to the summer period, reflecting patterns in both mixing depth and freshwater discharge.

Chl *a* concentrations reached their seasonal maxima in late April in the EGoF (up to 78 mg m^{-3}), and in early May in the INE and the NB (up to 42 mg m^{-3} in NB, Fig. 3c). After the spring bloom, regional Chl *a* maxima were typically located in the INE. In the eastern parts of the estuary concentrations remained rather constant throughout the summer varying between 9 and 12 mg m^{-3} in the NB and between 15 and 20 mg m^{-3} in the INE. In other regions, concentrations were more variable with 5–22 mg m^{-3} in the ONE and 4–11 mg m^{-3} in the EGoF, with a summer minimum in early summer (May–June) and a maximum in the peak of summer (July–August).

3.3. N and P pools

Concentrations of TN varied from 23 to 81 μM and DIN varied from the detection limit to 46 μM (Fig. 3d, e). In the NB, maxima of these nitrogen fractions were observed in early April, after which concentrations of TN and DIN decreased to relatively stable levels around 51 and 23 μM, respectively. In the EGoF, concentrations of TN ranged from 23 to 44 μM and DIN from below the detection limit to 13 μM.

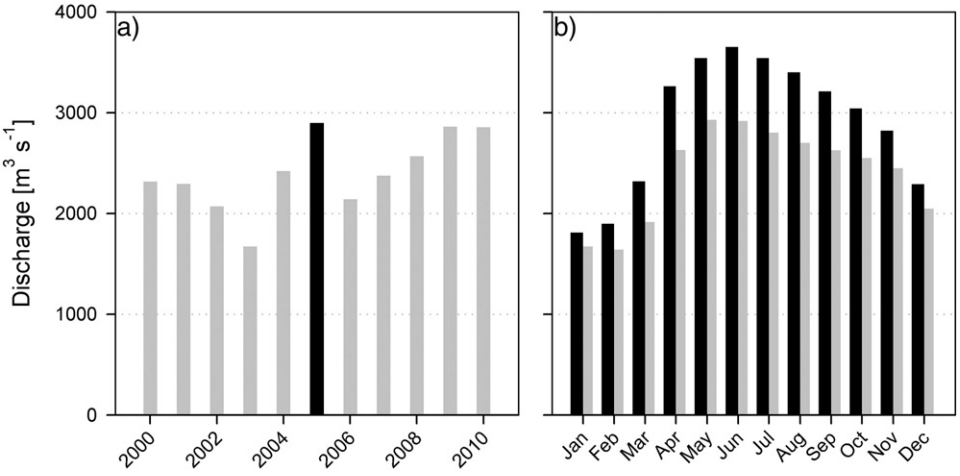

Fig. 2. a) Annual discharges between 2000 and 2010, and b) monthly discharges in 2005 (black bars) and corresponding mean discharges between 2000 and 2010 (grey bars) (Sergey Kondratyev, pers. comm.).

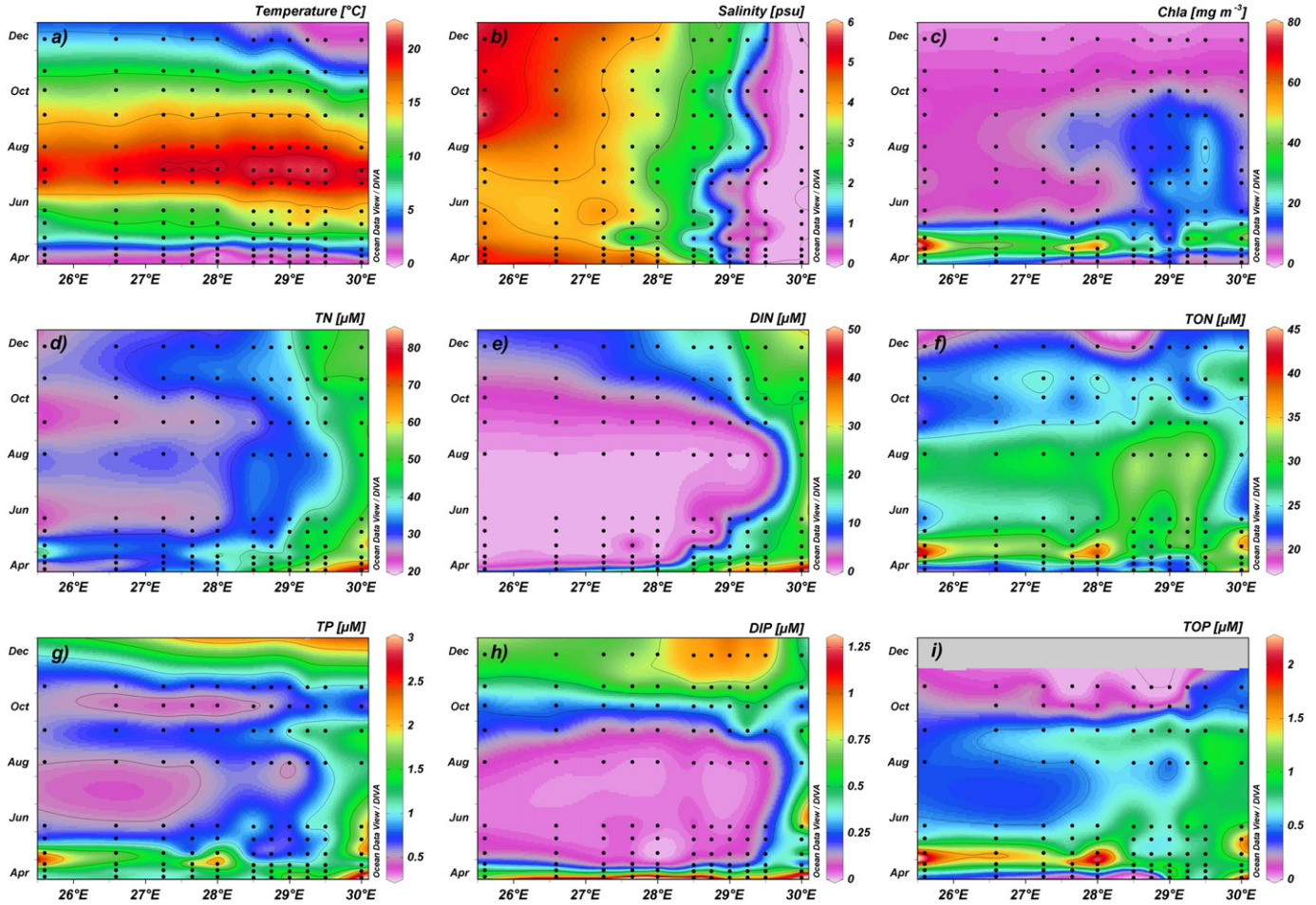

Fig. 3. Spatial and seasonal variation of a) temperature, b) salinity, c) Chl *a*, and various nutrient fractions: d) TN, e) DIN, f) TON, g) TP, h) DIP, and i) TOP. Black makers indicate sampling times and locations.

The concentration of organic nitrogen varied 18–43 μM (Fig. 3f), amounting to 42–100% of TN. The proportion of organic nitrogen varied both spatially and seasonally, lowest during mid-April (from 42% in the NB up to 65–82% in the EGoF), and highest during the late spring and summer (from 61% in the NB up to 100% in the EGoF). Concentrations of DON and PON ranged 12–24 μM (Fig. 4e; Table 1) and 3.8–25 μM (not plotted), respectively. The contribution of DON to TN, TDN, and TON increased typically from the NB (25–32, 25–43, and 48–56%) towards the EGoF (43–85, 64–99, and 43–86%), respectively. Concentrations of PON were closely related to Chl *a* ($r = 0.78$, $p < 0.0005$), whereas no such trend was observed for DON. DON concentrations increased from NB (12–16 μM) towards ONE (16–24 μM), after which signs of an opposite pattern were observed towards the open Gulf of Finland. Differences in seasonal trends were also observed among the study areas (Fig. 4e). DON at the stations closest to the river mouth declined from spring (~16–19 μM) towards autumn (~13 μM), whereas at other stations, concentrations increased during the spring. At the two westernmost stations, concentrations increased from early April to late May (from ~16–17 to ~19 μM), whereas at all middle stations the increase continued at least until early June (from ~14–19 μM to ~21–24 μM). Towards autumn, DON concentrations generally declined towards levels that prevailed in early spring.

Concentrations of TP ranged from 0.41 to 2.9 μM, and DIP from the detection limit up to 1.30 μM (Fig. 3g, h). The contribution of different phosphorus fractions to TP varied widely between the sea areas. In the NB, where all phosphorus pools were always present at detectable concentrations, the proportion of TOP to TP varied 44–85% (average 64%). The concentration of TOP (Fig. 3i) was closely correlated to Chl *a* in the EGoF ($r = 0.91$, $p < 0.0005$). This relationship weakened moving through the ONE ($r = 0.86$, $p < 0.0005$), and INE ($r = 0.52$, $p = 0.02$) into the NB (not significant).

Molar N/P ratios of total nutrients varied from 18 to 71, whereas clearly wider ranges were noted for inorganic (1.1–243) and organic (18–822) nutrients. In the NB, N/P ratios of both dissolved inorganic and organic nutrients were always well above the Redfield ratio of 16 with 28–136 and 20–60 for inorganic and organic nutrients, respectively. In contrast, the ratio of dissolved inorganic nutrients in the EGoF was generally below the Redfield ratio (1.1–133, median 9.6), while for organic nutrients it was always above Redfield (18–307).

3.4. DOM

CDOM absorption, ranging 2.70–17.8 m^{-1} at 350 nm, showed clear spatial and seasonal patterns (Table 1, Fig. 4a & 5a). In the NB, the $a_{CDOM}(350)$ minimum (7.58 m^{-1}) occurred in early April and the maximum (17.8 m^{-1}) in late April. After this maximum, $a_{CDOM}(350)$ decreased until early June to remain relatively constant level (around 10 m^{-1}) throughout the rest of the year. At the westernmost station of the EGoF, less distinct patterns were observed, with a slightly increasing trend from early April (4.17 m^{-1}) to early July (5.34 m^{-1}), whereas clearly lower absorptions (2.70–3.27 m^{-1}) were observed in autumn.

When calculated over the 300–700 nm wavelength range, slopes of the absorption curves varied from 14.3 to 21.2 μm^{-1} (Fig. 4b & 5b, Table 1). When S_{CDOM} was calculated over the wavelength range 400–700 nm, values were in a narrower range at 15.6–18.7 μm^{-1}. The ratio

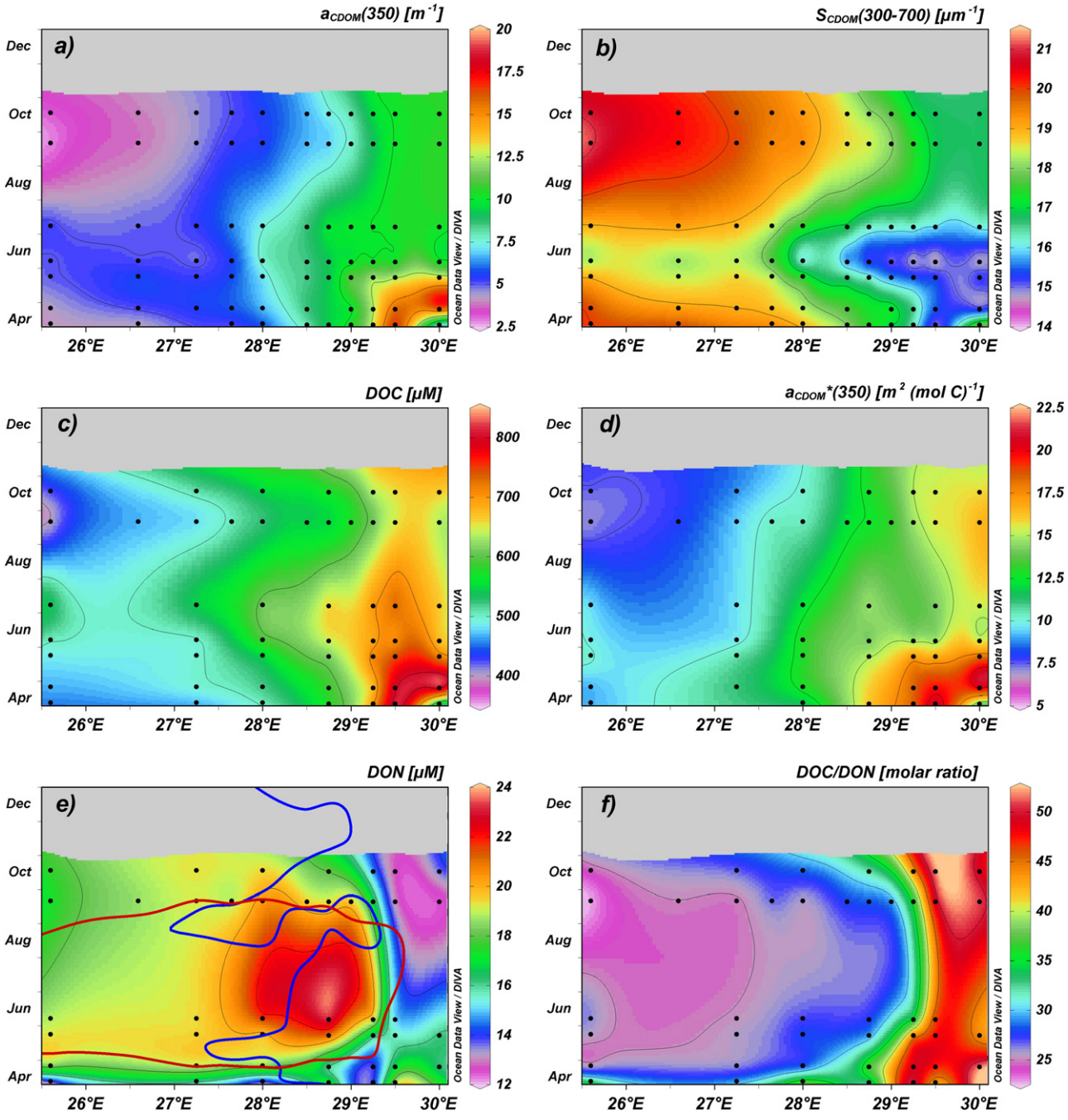

Fig. 4. Spatial and seasonal variation of a) $a_{CDOM}(350)$, b) $S_{CDOM}(300–700)$, c) DOC, d) $a_{CDOM}^*(350)$, e) DON, and f) molar DOC/DON. Black markers as in Fig. 3. Seasons and regions with potential phosphorus limitation are defined based on molar DIN/DIP ratios >16 (east of the blue line) and DIP concentration < 0.2 µM (west of the red line), following Fisher et al. (1992). (For interpretation of the references to color in this figure legend, the reader is referred to the web version of this article.)

Table 1
Properties of DOM, given as averages and ranges in parentheses for each sub-region (acronyms as in Fig. 1).

	This study					Aarnos et al. (2012)
Region	All	EGoF	ONE	INE	NB	NB
$a_{CDOM}(350)$ [m^{-1}]	7.90 (2.70–17.8)	5.21 (2.70–8.02)	8.69 (6.55–12.1)	11.6 (8.83–16.7)	11.4 (7.58–17.8)	10.3 (8.21–12.1)
$a_{CDOM}(442)$ [m^{-1}]	1.50 (0.464–3.77)	0.895 (0.464–1.59)	1.67 (1.17–2.46)	2.34 (1.70–3.47)	2.28 (1.39–3.77)	1.89 (1.38–2.29)
$S_{CDOM}(300–700)$ [μm^{-1}]	17.6 (14.3–21.2)	19.0 (15.4–21.2)	17.0 (14.8–18.6)	16.0 (14.3–17.4)	16.1 (14.4–18.0)	18.3 (17.8–19.1)
$S_{CDOM}(400–700)$ [μm^{-1}]	17.3 (15.6–18.7)	18.0 (17.1–18.7)	17.0 (16.2–17.9)	16.4 (15.7–16.9)	16.4 (15.6–16.9)	16.5 (16.1–17.1)
DOC [µM]	594 (390–840)	505 (390–612)	591 (539–666)	670 (598–814)	677 (551–840)	631 (584–684)
DON [µM]	17.3 (12.4–23.5)	18.9 (16.2–22.7)	19.2 (15.6–23.5)	15.6 (12.7–20.9)	14.6 (12.4–16.2)	15.1 (14.5–15.6)
$a_{CDOM}^*(350)$ [m^2 (mol C)$^{-1}$]	13.3 (6.94–21.2)	10.1 (6.94–13.3)	13.8 (12.1–16.1)	16.5 (14.0–20.6)	16.5 (13.8–21.2)	16.2 (14.1–17.7)
DOC/DON [mol:mol]	35.4 (22.6–51.9)	27.0 (22.6–29.2)	30.6 (27.7–37.6)	45.3 (32.2–51.7)	48.8 (43.5–51.9)	40.3 (37.5–43.0)

of S_{CDOM}(300–700) over S_{CDOM}(400–700) increased with salinity, with both slope ranges showing similar values at the lowest salinities, while for salinities over 4 values of S_{CDOM}(300–700) were typically higher than S_{CDOM}(400–700).

Despite commonly observed inverse relationships between S_{CDOM}(300–700) and $a_{CDOM,}$ changes of these variables were not always spatially and seasonally coupled. Anomalies were most apparent in the NB in early June, coinciding with maximum discharge of the Neva River. During this period, S_{CDOM}(300–700) remained near its seasonal minimum, despite a decline in a_{CDOM}(350) (Fig. 4a, b).

DOC concentrations varied from 390 to 840 μM and showed similar spatial and seasonal patterns to a_{CDOM}(350) (Figs. 4a, c & 5a, c). DOC concentrations were tightly related to both a_{CDOM}(350) ($r^2 = 0.94$, $p < 0.0005$) and a_{CDOM}(442) ($r^2 = 0.95$, $p < 0.0005$), and could be described by the nonlinear models below, reflecting differences in the behavior of DOC and a_{CDOM} over the study transect (Fig. 6a, b).

$$DOC = 176 + 132 \times a_{CDOM}(350)^{0.560} \quad (3)$$

$$DOC = 238 + 285 \times a_{CDOM}(442)^{0.561} \quad (4)$$

Three-fold variability was observed in $a_{CDOM}{}^{*}$(350), ranging 13.8–21.2 m^2 (mol C)$^{-1}$ in the NB to 6.94–13.3 m^2 (mol C)$^{-1}$ in the EGoF (Figs. 4d & 5d). In addition to a clear westward decreasing trend, $a_{CDOM}{}^{*}$(350) followed seasonal patterns parallel to a_{CDOM}, seen as the tight relationship between these variables (Fig. 6c). The overall variability in $a_{CDOM}{}^{*}$(350) was also clearly expressed in S_{CDOM} calculated over the wavelength ranges of 300–700 ($r = -0.831$, $p < 0.0005$) and 400–700 nm ($r = -0.850$, $p < 0.0005$).

The molar C/N ratio of DOM, ranged 22.6 to 51.9 (Fig. 4f) and decreased linearly with salinity ($r = -0.897$, $p < 0.005$). Overall variability of this ratio was dominated by spatial (CV ~26–31%) rather than seasonal variation (CV ~5–8%), the latter showing notable variability (CV ~12–17%) only at two sites in the INE and ONE. A strong positive relationship between DOC and DON was observed at the two easternmost sites ($r^2 = 0.772$, $p < 0.001$, slope ~32) and (albeit weaker) in the EGoF ($r^2 = 0.612$, $p < 0.001$, slope ~27) (Fig. 7). Regional differences in slopes were, however, not statistically significant. Between these areas, an abrupt change in this relationship was observed. This appears to be related to the increase in DON concentrations within the INE and ONE during summer (Fig. 4e & 5d), without a corresponding increase in DOC.

Effects of conservative and non-conservative processes on DOM distribution were evaluated based on the relationships of a_{CDOM}, S_{CDOM}, DOC, and DON with salinity (Fig. 5). When individual transects were considered, several spatial patterns deviating from conservative mixing models fitted over the whole salinity gradient were apparent. Residuals of mixing models showed 1 or 2 prominent discontinuity points in most salinity gradients. The positions of these discontinuity points varied seasonally, occurring at salinities ~1–4 PSU. Regarding a_{CDOM}(350) and DOC, values observed in the estuary were generally lower than expected from the mixing model in April, coinciding with the a_{CDOM} and DOC maximum at the river source. During the late spring to early summer period, when DOM concentrations at the river source were decreasing, values higher than expected from the mixing model typically observed in the estuary. The best match between observed distributions and conservative mixing models took place in autumn, after stabilization of a_{CDOM}, S_{CDOM}, and DOC concentrations at the river source close to their annual medians. During the same period, however, S_{CDOM} values in the estuary were clearly higher than expected from the mixing model. As expected, a strong negative relationship occurred between residuals of a_{CDOM} and S_{CDOM} ($r = -0.789$, $p < 0.001$). Furthermore, residuals of DOC had a clear positive correlation with a_{CDOM} ($r = 0.872$, $p < 0.001$) and weaker negative correlation with S_{CDOM} ($r = -0.560$, $p < 0.001$). Seasonal patterns in residuals of DON showed negative deviations at low salinities during spring and positive during the period extending from late spring to autumn. Residuals of DON had a positive correlation with DOC ($r = 0.622$, $p < 0.001$) and a_{CDOM} ($r = 0.309$, $p < 0.05$).

3.5. Loadings from the Neva River

Seasonal coverage of the available nutrient data allowed calculation of new loading estimates for several water constituents, noting that: (1) total and inorganic nutrient fractions were not measured in winter months, when lower flow rates (approximately half the average discharge between April and December) compensate for approximately twofold higher nutrient concentrations (Kuuppo et al., 2006); (2) DOC and DON concentrations were not measured as frequently as total and inorganic nutrient fractions but were characterized by low variability on a monthly basis (633–704 μM and 12.4–16.2 μM, respectively). The impact of these gaps in monthly nutrient data on our loading estimates was found to be minor (Supplement 1), with the highest uncertainty associated with loading estimates of TP, DIP, and NH4 (10–12% underestimation) and lowest uncertainty associated with TN and NO_{2+3} estimates (3.7 and 0.8% overestimation, respectively).

Calculated solely based on the measured data, TN and TP loads carried by the Neva River into the Gulf of Finland were estimated at 73.7 and 4.2 Gg yr^{-1}, respectively. Dissolved inorganic nitrogen and phosphorus pools contributed 29.8 (NO_{2+3}), 5.1 (NH_4) and 1.7 (DIP) Gg yr^{-1} (Table 2). TON and TOP loads therefore amounted to 38.8 and 2.6 Gg yr^{-1}, respectively. Annual DON load was also separately calculated at the easternmost site of the INE. DON concentrations here did not deviate significantly from those measured in the NB (*t*-test: $p = 0.297$), but had better seasonal coverage than in the NB. This estimate of DON load was 19.0 Gg yr^{-1}, and was close to the 17.4 Gg yr^{-1} based on concentrations in NB. Thus, annual PON load was 19.8 Gg yr^{-1}.

4. Discussion

4.1. Nutrients and chlorophyll-a

Present results support previous findings from the study area showing that algal production and biomass in the easternmost parts of the Neva estuary are generally limited by light and phosphorus, and by nitrogen in the EGoF (Pitkänen and Tamminen, 1995; Tamminen and Andersen, 2007). During the early spring, nutrient concentrations were high throughout the salinity gradient, and algal production was likely limited by light. Following exhaustion of the winter nutrient supply, primary production in summer relied on nutrients from river discharge and in situ regeneration. Dissolved inorganic nutrients carried by the river were transformed effectively into phytoplankton biomass during summer, and phosphorus depletion was evident at salinities <3, restricting any substantial production to the INE and ONE region. Low DIP concentrations (<0.2 μM) and DIN/DIP ratios generally above Redfield (>16) in these areas during summer months suggest phosphorus limitation (defined following Fisher et al., 1992). In contrast, DIN/DIP ratios in the EGoF were below the Redfield (<16), suggesting nitrogen limitation. In the NB, nutrient-replete conditions and light-limited growth persisted throughout the season. Accumulation of phytoplankton biomass in the NB is, on the other hand, limited by short residence times (2–7 days, Golubkov, 2009).

Efficient transformation of inorganic nutrients into phytoplankton biomass in the estuary is further emphasized by tight relationships of

Fig. 5. Variability of a) a_{CDOM}(350), b) S_{CDOM}(300–700), c) DOC, and d) DON concentrations along the salinity gradient. Black circles represent seasonal medians of these properties in NB. Dashed lines in a–d) represent mixing models based on freshwater and seawater end-members. The white background in each plot covers the environmental conditions defined by mixing models based on upper and lower limits of the freshwater end-member and the most representative case of the EGoF end-member. Non-filled black stars in y-axis represents levels observed in the NB during March 2007, June 2006, and September 2006 (Aarnos et al., 2012). Residuals of mixing models are presented in panels e–h.

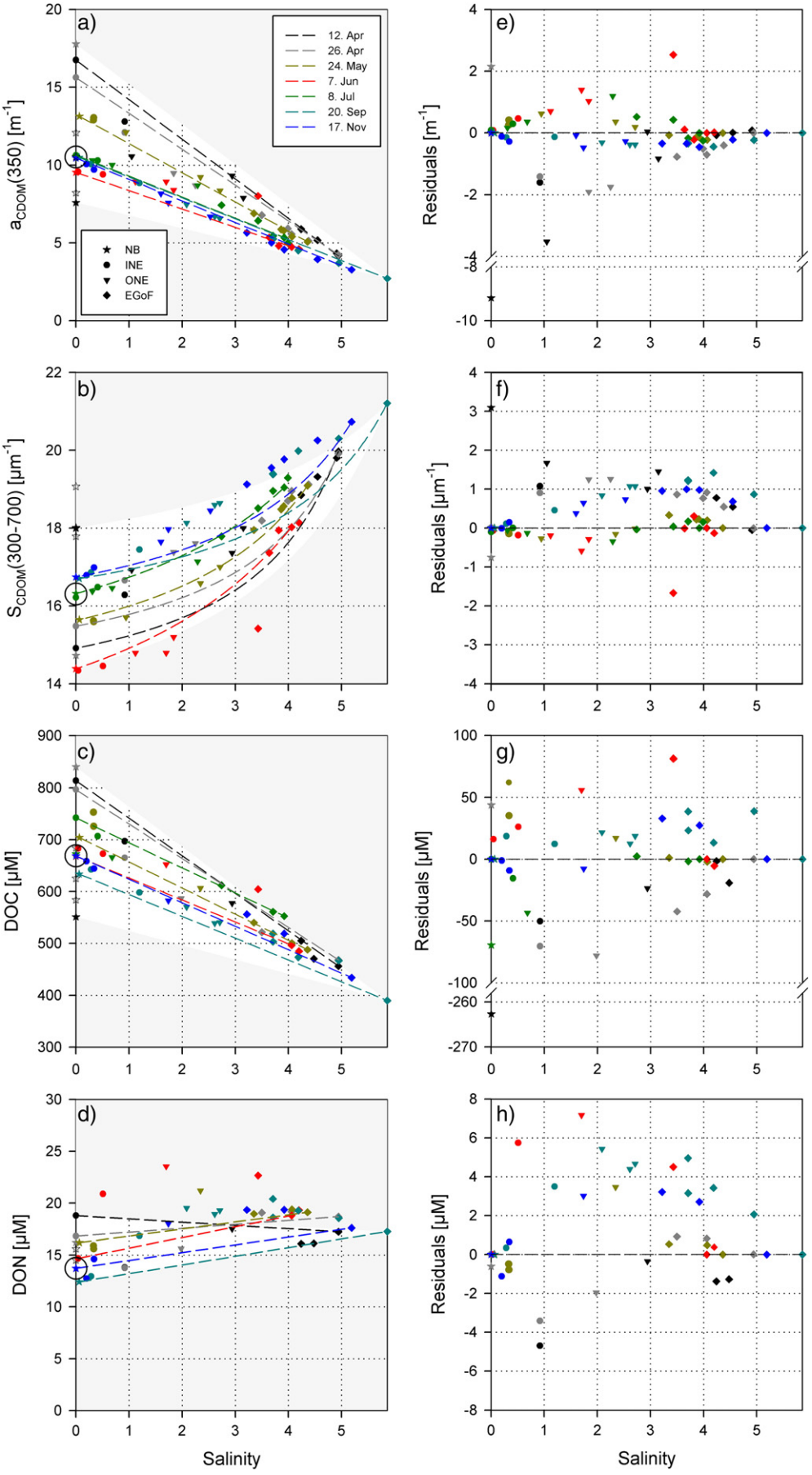
a)
12. Apr
26. Apr
24. May
7. Jun
8. Jul
20. Sep
17. Nov
NB
INE
ONE
EGoF
$a_{CDOM}(350)$ [m^{-1}]
e)
Residuals [m^{-1}]
b)
$S_{CDOM}(300\text{-}700)$ [μm^{-1}]
f)
Residuals [μm^{-1}]
c)
DOC [µM]
g)
Residuals [µM]
d)
DON [µM]
h)
Residuals [µM]
Salinity
Salinity

both PON and TOP with Chl *a*. No such relationship was observed between DON and Chl *a*, suggesting that production of phytoplankton biomass and DON in the estuary were spatially and seasonally uncoupled. Contributions of DON to TN and TON were low in the NB, compared to rivers discharging to the Baltic Sea, ranging 24–88% and 51–94%, respectively (Stepanauskas et al., 2002). Although contributions of different phosphorus pools were not determined in our study, the spatial differences in relationships between TOP and Chl *a* emphasize an increasing contribution of phosphorus, either in the dissolved organic pool or bound to non-algal particles, towards the river mouth.

4.2. DOM dynamics

4.2.1. DOC and DON

A significant positive relationship was previously observed between DOC and DON concentrations in Finnish river and streams (Mattsson, 2010). Here, such a relationship was also observed at the two stations closest to river mouth of the Neva River, and in the EGoF. However, when the whole study area is considered, concentrations of DOC and DON were clearly uncoupled. Based on DOC - DON relationship changes along the salinity gradient, three dynamically distinct regions were identified. Relationships are affected by mixing and are therefore dependent on concentrations at mixing end-members, but may also reflect regional changes in DOM dynamics, in this case suggesting a higher net loss of DOC relative to DON in area extending from NB to easternmost parts of INE (ΔDOC/ΔDON ~32) compared to EGoF (ΔDOC/ΔDON ~27), and net production of DON in the area stretching from the westernmost parts of the INE to the ONE.

DOM accumulation is often associated with phytoplankton bloom events and especially during their rapid transitions from a nutrient-replete to a nutrient limited stage (Carlson and Hansell, 2015). The quantity, quality, and subsequent pathways of organic matter produced during blooms, can vary due to a number of controlling factors, e.g. phytoplankton community structure, nutrient availability and type of nutrient limitation (Heiskanen and Kononen, 1994; Conan et al., 2007; Carlson and Hansell, 2015; Spilling et al., 2015). Autochthonously produced DOM could be released several complementary processes: extracellular release, grazer-mediated release and excretion, cell lysis, solubilization of detrital particles, and release from prokaryotes (Carlson and Hansell, 2015).

In the present study, accumulation of DON was observed in a wide region reaching from INE to EGoF, following spring bloom. Even more substantial accumulation occurred in summer albeit in a more restricted area extending from westernmost parts of INE to ONE, roughly corresponding to the zone where phosphorus was the limiting nutrient. Seasonal differences in DOM accumulation could relate to differences in the composition of phytoplankton community defining partly the fate of the organic matter produced (Heiskanen and Kononen, 1994). During spring it was dominated by diatoms in easternmost parts, and co-dominated by diatoms and dinoflagellates in westernmost parts of the study area, whereas during summer Cryptomonads, Chlorophytes, and Cyanophytes were more abundant.

Despite significant production of DON within the estuary, a comparable increase in DOC was not noted, probably due to stoichiometric changes in DOM from phytoplankton and differences in loss processes of DOC and DON. Nutrient availability has been shown to affect the production and composition of autochthonous DOM. In mesocosm experiments of Conan et al. (2007), 22–33% of the net production accumulated as DOC, showing the highest values under N-limitation. Furthermore, 6–22% of the assimilated nitrogen was recovered as DON in N-replete conditions, whereas during N-limitation, DON production is very low. During N-deficient conditions, molar C/N ratio of new DOM ranged between 35 and 90, but was constrained between 20 and 44 when inorganic nitrogen was available. Bioavailability of DON is generally considered to be higher compared to DOC, which affects the turnover time of these pools (Seitzinger et al., 2002; Wiegner et al., 2006). In the open Baltic Sea proportion of DON to TN is often high and could therefore be an important nitrogen source for plankton, especially during periods of DIN depletion (Vähätalo and Zepp, 2005). However, significance of DON as a nitrogen source of plankton could vary depending on availability of inorganic nitrogen. High dissolved inorganic nitrogen concentrations could reduce the utilization of DON (Kaushal and Lewis, 2005). Due to high DIN concentrations in the estuary, DON originating either from river or local production is mostly exported out from the estuary, enhancing productivity in the open Gulf of Finland. Furthermore, photochemical processes have been shown to mineralize DOC more efficiently than DON, especially in low-saline waters (Stedmon et al., 2007; Aarnos et al., 2012; Xie et al., 2012). In the Baltic Sea, the C/N ratios of photodegraded DOM varied from 112 in NB to 19 in the Arkona Basin, deviating markedly from the C/N ratio of bulk DOM in NB, but approximating this in the Arkona Basin (Aarnos et al., 2012). A similar change in DOM stoichiometry during photodegredation has also been reported within the salinity gradient of the Beaufort Sea (Xie et al., 2012), suggesting that photochemical transformation of DOM is likely a major contributor to the overall decrease in C/N ratio of DOM observed in coastal waters (Aarnos et al., 2012).

4.2.2. Spatial and seasonal changes in optical properties of DOM

The optical properties of DOM (high $a_{CDOM}^*(350)$ and generally low $S_{CDOM}(300–700)$) in the NB reflect the catchment properties of the Neva River with high contributions of forests, peatlands, and lakes. $S_{CDOM}(300–700)$ in the NB exhibited a much wider range than reported for three Finnish rivers discharging into the Baltic Sea (Asmala, 2014). The difference can be attributed to the influence of the large lakes within the Neva River catchment, leading to more diverse DOM. High $S_{CDOM}(300–700)$ and low a_{CDOM}^* observed in NB in early spring as well as during late summer and autumn, suggest that the riverine load consisted mainly of already partially transformed DOM from Lake Ladoga. Low $S_{CDOM}(300–700)$ and high a_{CDOM}^* during the late spring and early summer, instead, suggest higher contribution of fresh DOM, drained from surrounding land. In contrast to $S_{CDOM}(300–700)$ remained low and at a rather constant level from late April to early July, $a_{CDOM}(350)$ and DOC decreased from late April to early June, indicating a dilution of river water over a period of increasing river flow. This was likely related to changes in flow paths of runoff and a balance between soil processes, e.g. leaching, desorption, and adsorption (Kortelainen et al., 2004). In EGoF, observed a_{CDOM}, S_{CDOM}, and a_{CDOM}^* values were consistent with those previously reported by Stedmon et al. (2007) for their sampling station in the EGoF (60°15′N, 27°15′E; August 2005). Compared to the NB, $a_{CDOM}(350)$ and DOC in the EGoF clearly reached their seasonal maxima later. Nevertheless, low $S_{CDOM}(300–700)$ coinciding with these maxima suggest common, predominantly allochthonous origins of both peaks. Lowest $a_{CDOM}(350)$ and highest $S_{CDOM}(300–700)$ values in both NB and EGoF were observed in autumn. Contrary to the study of Kowalczuk et al. (2010), a clear seasonal pattern was also observed in $a_{CDOM}^*(350)$, especially in the vicinity of the river mouth, where the highest values were observed during the period of increasing the river flow, reflecting a high contribution of fresh DOM during this period.

Various production and loss processes of DOM have been shown to lead to changes in optical signatures of DOM specific to particular process (e.g. Helms et al., 2008; Fichot and Benner, 2012; Yamashita et al., 2013; Asmala et al., 2014). Increase of S_{CDOM} especially at the wavelength range of 275–295 nm are often related to photochemical degradation of terrestrial DOM (Helms et al., 2008; Fichot and Benner, 2012). Photochemical decomposition of DOM is highest during the summer months when solar radiation and water temperatures are highest (Aarnos et al., 2012) explaining higher slopes observed in late summer and autumn. Plankton derived DOM could also contribute to higher $S_{CDOM}(275–295)$, although experimental additions of plankton-produced DOM to coastal samples have shown only moderate effects (Fichot and Benner, 2012). Furthermore, a considerable part of

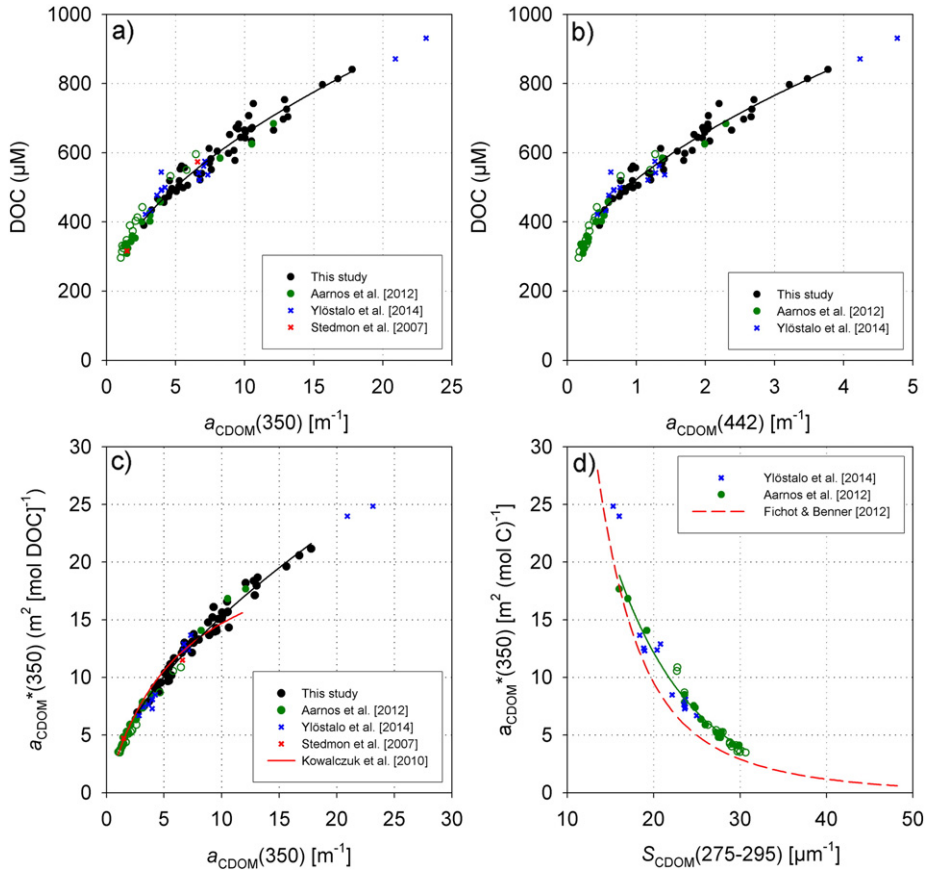

Fig. 6. Relationships between DOC and a) $a_{CDOM}(350)$ and b) $a_{CDOM}(442)$, c) between a_{CDOM}*(350) and $a_{CDOM}(350)$ and d) between a_{CDOM}*(350) and $S_{CDOM}(275–295)$. Black symbols and lines represent data and relationships from the present study. Red symbols represent data from the Gulf of Finland and Arkona Sea (Stedmon et al., 2007), blue symbols from lakes of southern Finland (Ylöstalo et al., 2014), filled green symbols represent unbleached samples collected from a transect from the Neva Bay to the Arkona Sea, and open green symbols represent the same samples exposed to irradiation (reprocessed from Aarnos et al., 2012). Continuous and dashed red lines denote relationships from the Baltic Sea (Kowalczuk et al., 2010) and coastal waters of the Gulf of Mexico (Fichot and Benner, 2012), respectively. (For interpretation of the references to color in this figure legend, the reader is referred to the web version of this article.)

autochthonous DOM is labile and therefore consumed and respired rapidly by the microbial community. Microbial degradation with a contrasting effect on $S_{CDOM}(275–295)$ could also largely outbalance the effects of autochthonous DOM (Helms et al., 2008; Fichot and Benner, 2012). The observed relationship between a_{CDOM}*(350) and $S_{CDOM}(275–295)$ in the Baltic Sea (reprocessed from Aarnos et al., 2012) clearly emphasizes the importance of photochemical processes among various transformation processes of CDOM in the Baltic Sea. This result is consistent with reports from coastal waters of the Gulf of Mexico (Fichot and Benner, 2012) and Finnish lake waters (Ylöstalo et al., 2014).

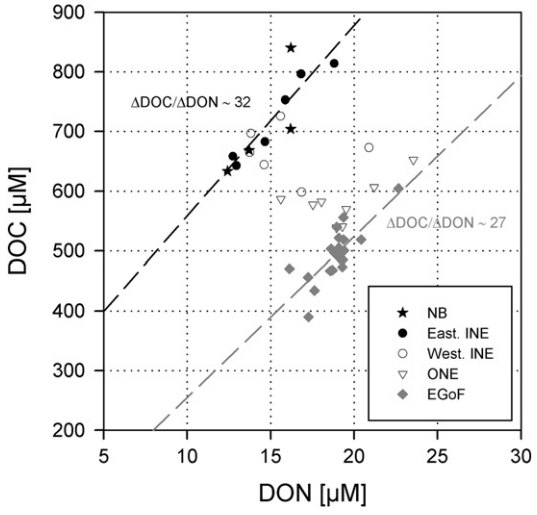

Fig. 7. Relationship between DOC and DON along the study transect from the NB to the EGoF. ΔDOC/ΔDON was approximately 32 ($r^2 = 0.772$, $p < 0.001$) in the area extending from the NB to the easternmost parts of INE (black filled symbols) and value of ~27 ($r^2 = 0.612$, $p < 0.001$) in the EGoF (grey filled symbols).

4.3. Estuarine mixing dynamics

In dynamic systems like estuaries, strong seasonality in the freshwater end-member(s) complicates the interpretation of mixing patterns (Loder and Reichard, 1981, Bowers and Brett, 2008). Depending on the balance between estuarine flushing time and the timescale of source variation (e.g. river discharge and CDOM concentration), non-linear relationships between water constituents and salinity may exist even in case of purely conservative mixing (Bowers and Brett, 2008). In estuarine mixing models, both end-members are generally considered independent. It is, however, clear that DOM in coastal waters carries also history from its freshwater source and its transformations during estuarine transport and vice versa. Therefore, data of separate transects should always be considered merely as snapshots of DOM distribution in the estuary. As the flushing time of the estuary gets longer, changes in the properties of the river source are reflected further from the river mouth only after an increasing lag period. Within the estuary, this could be seen as values higher than expected by mixing model

Table 2
Loading estimates of nitrogen, phosphorus and carbon pools (Gg yr^{-1}) from the River Neva and St. Petersburg (loadings from the Neva River alone are given in parentheses).

	This study	Kondratyev and Trumbull (2012)	Kuuppo et al. (2006)	Kiirikki et al. (2003)	Stålnacke et al. (1999)	Kuliński and Pempkowiak (2011)	Kondratyev et al. (2004)
Study period	2005	2005	2001	2000	1980–1993	not given	1991–93, 1996–98
TN	73.5	65.3[d] (53.1)	(45.2)	56.2[c] (43.0)	(55.6)		
TP	4.2	3.2[d] (1.3)	(1.9)	3.1[c] (1.3)	(3.2)		
$NO_2 + NO_3$	29.8		(17.3)		(21.2)[b]		
NH_4	5.1		(3.2)				
DIP	1.7		(0.52)		(1.2)		
TOC	789–824[a]					(1210)[e]	(603)
TON	38.8		(24.7)				
TOP	2.6		(1.4)		(2.0)		
DOC	741						
DON	19.0		(19.4)				
PON	19.8		(5.3)				

[a] Calculated assuming DOC = 0.94–0.90*TOC (Mattsson, 2010; Heikkinen, 1989).
[b] Includes only NO_3.
[c] Calculated as sum of loading from the Neva River and waste waters from St. Petersburg.
[d] Calculated as sum of loadings from Lake Ladoga into the Neva River and from wastewater treatment plants of St. Petersburg (data digitized from figures).
[e] Estimate based on data of two adjacent rivers, Virojoki and Narva.

when the properties of the river decrease, or lower than expected when these properties of the river water increase. Such patterns can easily be misinterpreted as non-conservative, e.g. caused by local loss and production processes, especially when deduced from spatially and seasonally scarce data and without knowledge of the variability of the river source. Good fit between observed DOM distribution and modelled distribution are expected when time scale of source variation compared to flushing time of the estuary is either very short or large.

Jönsson et al. (2011) proposed based on lagrangian-trajectory analysis that the most pronounced mixing of water masses originating from the Northern Baltic Proper and the Neva River takes place in the easternmost parts of Gulf of Finland, over a narrow zone which position and extent vary over time. The exact location of this zone between 27 and 29°E (i.e. a salinity range 1–4 PSU), appears to be intricately controlled and is neither linked to freshwater flux nor wind forcing alone (Jönsson et al., 2011). This transient zone between the water masses is consistent with the observed discontinuities visible in the salinity relationships of $a_{CDOM}(350)$ in our study, suggesting that the observed deviations from the mixing model reflect combined effects of seasonal variations in the properties (excluding salinity) of the freshwater end-member, and differences in the age of water masses within the estuary, the latter governed by the specific mixing dynamics of this estuary.

The fact that nearly all our estuarine observations (excluding DON) fall between upper and lower bounds of all possible mixing lines demonstrates that conservative mixing, when the seasonal variability in river source and mixing properties of particular estuary are considered, can explain the observed DOM distributions. On the other hand, a possible influence of non-conservative processes cannot be ruled out without detailed high-frequency observations. Reciprocally, observations falling clearly above or below these bounds would prove that non-conservative processes were involved. During the growth season DON concentrations in the estuary fall clearly above its upper bound, suggesting that its local production exceeded losses during this period. While observed distributions of a_{CDOM} (as well as DOC) agreed well to mixing model during the stabile period of river source, S_{CDOM} were still above mixing line emphasizing the effects of photochemistry on DOM quality. To verify the exact roles of non-conservative processes on spatial and seasonal dynamics of DOM in estuaries, data with higher spatial and seasonal resolution should be collected and compared with the data from hydrodynamic models.

4.4. Loadings into the Baltic Sea from the Neva River and St. Petersburg

4.4.1. Nitrogen and phosphorus

Loading estimates reported here are based on concentrations in NB, thereby integrating loads from the Neva River and the city of St. Petersburg. Some of the earlier studies shown in Table 2 (except Kiirikki et al., 2003 and Kondratyev and Trumbull, 2012) report only loads from the Neva River. Kondratyev and Trumbull (2012) report loads from wastewater treatment plants of St. Petersburg in the order of 12.3 Gg nitrogen and 2 Gg phosphorus (with molar N/P ratio 13.6) during 2005. Subtracted from our data, approximately 61.4 Gg of nitrogen and 2.2 Gg of phosphorus (with molar N/P ratio of 57.5) are left for other sources, originating mainly from the Neva River. If differences in flow rates between years are taken into account, our estimates on total N and P fluxes from the Neva River alone compare well against previous studies (Table 2). Less than half of the total N and P loads received by NB were in inorganic form, consistent with previous studies (Stålnacke et al., 1999; Kuuppo et al., 2006). However, we note a considerable difference in PON loads between our study and Kuuppo et al. (2006), whose estimates were approximately three times lower than those presented here. We note that the loading estimates of Kuuppo et al. (2006) were based exclusively on samples from the Neva River and transformation of dissolved inorganic nitrogen into particulate matter in the NB could therefore explain this inconsistency between studies. DON estimates, instead, were consistent, suggesting that contribution of St. Petersburg to DON load is relatively small compared to the load from the Neva River.

According to HELCOM (2012), the Baltic Sea received ca. 681 Gg N yr^{-1} and 33 Gg P yr^{-1}, and Gulf of Finland 82 Gg N yr^{-1} and 6.5 Gg P yr^{-1} as waterborne loads during the period 1994–2008. The Neva River and St. Petersburg would therefore contribute ca. 11% and 90% of the TN, and 13% and 64% of TP loads into the Baltic Sea and Gulf of Finland, respectively. Scaled to catchment area, annual nutrient loadings of TN and TP from the Neva River alone (219 and 7.64 kg km^{-2} yr^{-1}, respectively) were lower compared to catchments of the other major rivers discharging into the Baltic Sea (Vistula, Oder, Nemunas and Daugava), with loads ranging 594–798 (TN) and 15–56 (TP) kg km^{-2} yr^{-1} (Stålnacke et al., 1999), and similar to those reported for Finnish river catchments ranging 185–600 (TN) and 2.0–18.5 (TP) kg km^{-2} yr^{-1} (Mattsson et al., 2009; Asmala et al., 2013). Our area-

specific DON load (61.7 kg km^{-2} yr^{-1}), instead, was clearly lower than those of several Finnish river catchments (91–270 kg km^{-2} yr^{-1}, Mattsson et al., 2009).

4.4.2. Organic carbon

DOC concentrations in the NB were consistent with those previously reported for Lake Ladoga, ranging 670–800 μM (Kondratyev and Filatov, 1999; Ostapenia et al., 2009), suggesting that (in contrast to results for TN and TP) the contribution of St. Petersburg to DOC load is small compared to the load from the Neva River. Annual area-specific DOC load from the Neva River catchment (2.6 t km^{-2} yr^{-1}) falls in the lower end of the range reported for Finnish catchment areas (2.2–7.2 t km^{-2} yr^{-1}; Räike et al., 2012). The Neva River catchment contains several large lakes, which are known to affect the retention and transformation of organic matter (Drabkova et al., 1996). Our annual loading estimate is only slightly above the 2.1 t km^{-2} predicted by relating the percentage lake area in the catchment to area-specific loading (Räike et al., 2012). Our estimates closely resemble the area-specific loading of 2.3 t km^{-2} reported for the Finnish side of the Vuoksi river basin, comprising ca. 20% of the total catchment area of Neva River (Kondratyev, 2011; Räike et al., 2012).

A major part of TOC (90–95%) in boreal rivers as well as in small lakes (97 ± 5% in epilimnion) is in dissolved form (Heikkinen, 1989; Mattsson et al., 2005; von Wachenfeldt and Tranvik, 2008; Mattsson, 2010). As the Neva River receives most of its water from Lake Ladoga, phytoplankton production within this large lake could affect DOC/TOC ratio (as well as its seasonal variability) in the Neva River. Nevertheless, above range agrees well both with our unpublished measurements from the Neva Bay and proportion reported for Lake Ladoga (93%; Ostapenia et al., 2009). Our estimate of annual DOC loading from the Neva River would therefore correspond to TOC loads ranging from 789 to 824 Gg yr^{-1}. This is higher than the 603 Gg yr^{-1} estimated by Kondratyev et al. (2004), but clearly lower than 1210 Gg yr^{-1} used by Kuliński and Pempkowiak (2011) in their recent carbon budget of the Baltic Sea. It should be noted that the former estimate is based on measurements of chemical oxygen demand, while the latter is based on data from two relatively minor adjacent rivers (Narva and Virojoki) whose catchments differ from the Neva River catchment with regard to their lake percentages: 8% in Narva (UNECE, 2011) and 3% in Virojoki (Räike et al., 2012). Based on our estimate, the TOC load from Neva River corresponds to ca. 19–20% of the total load into the Baltic Sea, estimated as 4086 Gg yr^{-1} in Kuliński and Pempkowiak (2011) and 4256 Gg yr^{-1} in Gustafsson et al. (2014). On the other hand, our estimates of DOC load from the Neva River exceed the total load into the Gulf of Finland of the carbon flux model by Gustafsson et al. (2014), supporting their assumption that total DOC loading into the Gulf of Finland has been underestimated.

As our estimate for TOC load from the Neva River deviated significantly from the carbon budget of Kuliński and Pempkowiak (2011), we must evaluate how this difference affects the outcome of their carbon budget. According to the original model based on a mass balance approach, the Baltic Sea acts as a weak source of CO_2, releasing 1.05 (±1.71) Tg of carbon yr^{-1} into the atmosphere. Using our estimate for the TOC load from the Neva River, the total riverine TOC load into the Baltic Sea reduces to 3.40–3.44 Tg yr^{-1} (from 4.1 Tg yr^{-1} of original model), and the CO_2 emissions from the Baltic Sea into the atmosphere to 0.36–0.40 Tg of carbon yr^{-1}. When we further apply a correction for the flow rate of the River Kemijoki (564 m^3 s^{-1}, Räike et al., 2012), total riverine loads of TIC reduce to 6.57 Tg yr^{-1} (from 6.81 Tg yr^{-1} of the original model), and TOC to 3.54–3.58 Tg yr^{-1}, respectively. Applying these changes, CO_2 emissions from the Baltic Sea into the atmosphere reduce further to 0.26–0.30 Tg of carbon yr^{-1}. The corrected model thus yields a negligible contribution from the Baltic Sea to atmospheric CO_2 in relation to anthropogenic carbon emissions of its riparian countries, estimated as 337 Tg yr^{-1} (excluding Russia) in 2011 (Boden et al., 2013).

5. Conclusions

The share of the Neva River to total DOC and TOC loadings into the Baltic Sea follows its contribution to freshwater input, whereas its contribution to nitrogen and phosphorus loads amounts to only half of what is expected based on runoff. Despite its low area-specific nutrient loadings relative to other rivers draining into the Baltic Sea, loads from the Neva River and from the city of St. Petersburg have a major impact on the ecological state of the Neva estuary and Gulf of Finland, due to small size of the receiving basin compared to the large size of the river catchment. In contrast to loads of dissolved inorganic N and P, the contribution from St. Petersburg to DOC and DON loads is relatively small compared to loads from the Neva River catchment.

Seasonal variation in riverine DOM properties could lead to distribution patterns in the estuary, which can easily be misinterpreted as non-conservative processes. To draw conclusions from residuals of mixing models on the relative importance of local production and loss processes to DOM distribution in estuaries, seasonality in river source concentrations as well as hydrodynamics of the receiving estuary should be taken into account.

The spatial distribution of DOC and a_{CDOM} in the Neva estuary are governed by seasonal changes in riverine loads and estuarine mixing dynamics, mostly overriding the effects of local production and loss processes, of which photochemical processes appear to be most significant. DON distributions, instead, were clearly affected by local production in the estuary. DIN was effectively transformed in the estuary into PON and DON, of which DON was mostly exported out from the estuary, enhancing productivity in nitrogen limited parts of the Gulf of Finland.

Previous DOC loading estimates of this largest river of the Baltic Sea have been based on educated guesses rather than measurements. In this study, we demonstrate that such knowledge gaps significantly affect our understanding of the carbon balance in the Baltic Sea. It is important to define all key biogeochemical loading, mixing, and transformation processes before definitive conclusions on the role of the Neva and other rivers in the Baltic Sea carbon cycle can be drawn.

Acknowledgments

The authors thank Silja Line (presently part of the Tallink group) for access to their ship under the Alg@line network. We are also grateful to staff of Tvärminne Zoological Station for facilities and technical assistance and to Sergey Kondratyev (Institute of Limnology of the Russian Academy of Sciences) for providing runoff data of the Neva River. The authors gratefully acknowledge the contributions by anonymous reviewers and the associate editor, which helped to improve the manuscript. This study was funded by the Walter and Andrée de Nottbeck Foundation, and the Academy of Finland (SA104901).

Appendix A. Supplementary data

Supplementary data to this article can be found online at http://dx.doi.org/10.1016/j.marchem.2016.07.004.

References

Aarnos, H., Ylöstalo, P., Vähätalo, A.V., 2012. Seasonal phototransformation of dissolved organic matter to ammonium, dissolved inorganic carbon, and labile substrates supporting bacterial biomass across the Baltic Sea. J. Geophys. Res 117 (G01004), 2012. http://dx.doi.org/10.1029/2010JG001633.

Abril, G., Nogueira, M., Etcheber, H., Cabecadas, G., Lemaire, E., Brogueira, M.J., 2002. Behaviour of organic carbon in nine contrasting European estuaries. Estuar. Coast. Shelf Sci 54, 241–262.

Akkanen, J., Slootweg, T., Mäenpää, K., Leppänen, M.T., Agbo, S., Gallampois, C., Kukkonen, J.V.K., 2012. Bioavailability of organic contaminants in freshwater environments. Handbook of Environmental Chemistry. Vol. 19, pp. 25–54. http://dx.doi.org/10.1007/978-3-642-25722-3_2.

Andrejev, O., Myrberg, K., Lundberg, P.A., 2004. Age and renewal time of water masses in a semi-enclosed basin – application to the Gulf of Finland. Tellus 56A, 548–558.

Asmala, E., 2014. Transformation and removal of riverine dissolved organic matter in Baltic Sea estuaries PhD thesis Monographs of the Boreal Environment Research. Vol. 45.

Asmala, E., Autio, R., Kaartokallio, H., Pitkänen, L., Stedmon, C.A., Thomas, D., 2013. Bioavailability of riverine dissolved organic matter in three Baltic Sea estuaries and the effect of catchment land use. Biogeosciences 10, 6969–6986.

Asmala, E., Autio, R., Kaartokallio, H., Stedmon, C.A., Thomas, D., 2014. Processing of humic-rich riverine dissolved organic matter by estuarine bacteria: effects of predegradation and inorganic nutrients. Aquat. Sci 76, 451–463.

Bergström, B., Carlsson, B., 1994. River runoff to the Baltic Sea: 1950–1990. Ambio 23, 280–287.

Boden, T.A., Marland, G., Andres, R.J., 2013. Global, Regional, and National Fossil-Fuel CO_2 Emissions. Carbon Dioxide Information Analysis Center, Oak Ridge National Laboratory, U.S. Department of Energy, Oak Ridge, Tenn., U.S.A. http://dx.doi.org/10.3334/CDIAC/00001_V2013.

Bowers, D.G., Brett, H.L., 2008. The relationship between CDOM and salinity in estuaries: an analytical and graphical solution. J. Mar. Syst 73, 1–7.

Bronk, D.A., See, J.H., Bradley, P., Killberg, L., 2007. DON as a source of bioavailable nitrogen for phytoplankton. Biogeosciences 4, 283–296.

Carlson, C.A., Hansell, D.A., 2015. DOM sources, sinks, reactivity and budgets. In: Hansell, D.A., Carlson, C.A. (Eds.), Biogeochemistry of Marine Dissolved Organic Matter, second ed. Elsevier, pp. 65–126.

Conan, P., Søndergaard, M., Kragh, T., Thingstad, F., Williams, P.J.L.B., Markager, S., Cauwet, G., Borch, N.H., Evans, D., Riemann, B., 2007. Partitioning of organic production in marine plankton communities: the effect of inorganic nutrient ratios and community composition on new dissolved organic matter. Limnol. Oceanogr 52 (2), 753–765.

Drabkova, V.G., Rumyantsev, V.A., Sergeeva, L.V., Slepukhina, T.D., 1996. Ecological problems of Lake Ladoga: causes and solutions. Hydrobiologia 322, 1–7.

Elmgren, R., 2001. Understanding human impact on the Baltic ecosystem: changing views in recent decades. Ambio 30, 222–231.

Fichot, C.G., Benner, R., 2012. The spectral slope coefficient of chromophoric dissolved organic matter (S275–295) as a tracer of terrigeneous dissolved organic carbon in river-influenced ocean margins. Limnol. Oceanogr 57, 1453–1466.

Fisher, T.R., Peele, E.R., Ammerman, J.W., Harding, L.W., 1992. Nutrient limitation of phytoplankton in Chesapeake Bay. Mar. Ecol. Prog. Ser 82, 51–63.

Golitsyn, G.S., Efimova, L.K., Mokhov, I.I., Rumyantsev, V.A., Somova, N.G., Khon, V.C., 2002. Ladoga and Onega hydrological regimes and their variations. Water Res 29 (2), 149–154.

Golubkov, M.S., 2009. Phytoplankton primary production in the Neva Estuary at the turn of the 21st century. Inland Water Biol 2 (4), 20–26.

Gustafsson, E., Deutsch, B., Gustafsson, B.G., Humborg, C., Mörth, C.-M., 2014. Carbon cycling in the Baltic Sea – the fate of allochthonous organic carbon and its impact on air–sea CO_2 exchange. J. Mar. Syst 129, 289–302.

Häder, D.-P., Kumar, H.D., Smith, R.C., Worrest, R.C., 2007. Effects of solar UV radiation on aquatic ecosystems and interactions with climate change. Photochem. Photobiol. Sci 6, 267–285.

Hanssen, H.P., Koroleff, F., 1999. Determination of nutrients. In: Grasshoff, K., Kremling, K., Ehrhardt, M. (Eds.), Methods of Seawater Analysis. Weinheim, Wiley VCH, pp. 159–228.

Heikkinen, K., 1989. Organic carbon transport in an undisturbed boreal humic river in northern Finland. Arch. Hydrobiol 117, 1–19.

Heiskanen, A.-S., Kononen, K., 1994. Sedimentation of vernal and late summer phytoplankton communities in the coastal Baltic Sea. Arch. Hydrobiol 131, 175–198.

HELCOM, 1993. Second Baltic Sea pollution load compilation. Baltic Sea Environment Proceedings No. 45. HELCOM, Helsinki.

HELCOM, 2009. Eutrophication in the Baltic Sea – an integrated thematic assessment of the effects of nutrient enrichment and eutrophication in the Baltic Sea region. Baltic Sea Environ. Proc. 115B.

HELCOM, 2012. Fifth Baltic Sea pollution load compilation (PLC-5). Baltic Sea Environment Proceedings No. 128. HELCOM, Helsinki.

Helms, J.R., Stubbins, A., Ritchie, J.D., Minor, E.C., Kieber, D.J., Mopper, K., 2008. Absorption spectral slopes and slope ratios as indicators of molecular weight, source, and photobleaching of chromophoric dissolved organic matter. Limnol. Oceanogr 53, 955–969.

Johnson, K.S., Coletti, L.J., 2002. *In situ* ultraviolet spectrophotometry for high resolution and long-term monitoring of nitrate, bromide and bisulfide in the ocean. Deep-Sea Res. I Oceanogr. Res. Pap. 49, 1291–1305.

Jönsson, B.F., Döös, K., Myrberg, K., Lundberg, P.A., 2011. A lagrangian-trajectory study of a gradually mixed estuary. Cont. Shelf Res 31, 1811–1817.

Kaushal, S.S., Lewis, W.M., 2005. Fate and transport of organic nitrogen in minimally disturbed montane streams of Colorado, USA. Biogeochemistry 74 (3), 303–321.

Kiirikki, M., Rantanen, P., Varjopuro, R., Leppänen, A., Hiltunen, M., Pitkänen, H., Ekholm, P., Moukhametshina, E., Inkala, A., Kuosa, H., Sarkkula, J., 2003. Cost effective water protection in the Gulf of Finland. Focus on St. Petersburg. Finnish Environ 632, 1–55.

Kondratyev, K.Y., Filatov, N., 1999. Limnology and Remote Sensing: A Contemporary Approach. Praxis Publishing, UK, p. 406.

Kondratyev, S., Trumbull, N., 2012. Nutrient loading on the eastern Gulf of Finland (Baltic Sea) from the Russian catchment area. J. Hydrol. Hydromechan 60, 145–151.

Kondratyev, S.A., 2011. Estimation of the nutrient load on the Gulf of Finland from the Russian part of its catchment. Water Res 38, 63–71.

Kondratyev, S.A., Alyabina, G.A., Bovykin, I.V., Sorokin, I.N., 2004. Total organic carbon load on the Gulf of Finland from its Russian catchment area. Proc. Estonian Acad. Sci. Biol. Ecol 53, 106–115.

Kördel, W., Dassenakis, M., Lintelmann, J., Padberg, S., 1997. The importance of natural organic material for environmental processes in water and soils. Pure Appl. Chem 69 (7), 1571–1600.

Kortelainen, P., Mattsson, T., Laubel, A., Evans, D., Cauwet, G., Räike, A., 2004. Sources of dissolved organic matter from land. In: Søndergaard, M., Thomas, D.N. (Eds.), Dissolved Organic Matter (DOM) in Aquatic Ecosystems: A Study of European Catchments and Coastal Waters, the Domaine Project, pp. 15–22.

Kowalczuk, P., Stedmon, C.A., Markager, S., 2006. Modelling absorption by CDOM in the Baltic Sea from season, salinity and chlorophyll. Mar. Chem 101, 1–11.

Kowalczuk, P., Zabłocka, M., Sagan, S., Kuliński, K., 2010. Fluorescence measured *in situ* as a proxy of CDOM absorption and DOC concentration in the Baltic Sea. Oceanologia 52, 431–471.

Kuliński, K., Pempkowiak, J., 2011. The carbon budget of the Baltic Sea. Biogeosciences 8, 3219–3230.

Kuuppo, P., Tamminen, T., Voss, M., Schulte, U., 2006. Nitrogenous discharges to the eastern Gulf of Finland, the Baltic Sea: elemental flows, stable isotope signatures, and their estuarine modification. J. Mar. Syst 63, 191–208.

Leppänen, J.-M., Rantajärvi, E., 1995. Unattended recording of phytoplankton and supplemental parameters on board merchant ships – an alternative to the conventional algal monitoring programmes in the Baltic Sea. In: Lassus, P., Arzul, G., Erard-Le Denn, E., Gentien, P., T. & C. Marcaillore-Le Baut (Eds.), Harmful Marine Algal Blooms. Lavoisier Science, Paris, pp. 719–724.

Leppänen, J.-M., Rantajärvi, E., Hällfors, S., Kruskopf, M., Laine, V., 1995. Unattended monitoring of potentially toxic phytoplankton species in the Baltic Sea in 1993. J. Plankton Res 17 (4), 891–902.

Lignell, R., Hoikkala, L., Lahtinen, T., 2008. Effects of inorganic nutrients, glucose and solarradiation on bacterial growth and exploitation of dissolved organic carbon and nitrogen in the northern Baltic Sea. Aquat. Microb. Ecol 51, 209–221. http://dx.doi.org/10.3354/ame01202.

Loder, T.C., Reichard, R.P., 1981. The dynamics of conservative mixing in estuaries. Estuaries 4, 64–69.

Markager, S., Stedmon, C.A., Søndergaard, M., 2011. Seasonal dynamics and conservative mixing of dissolved organic matter in the temperate eutrophic estuary Horsens Fjord. Estuar. Coast. Shelf Sci 92, 376–388.

Mattsson, T., 2010. Export of organic matter, sulphate and base cations from headwater catchments downstream to the coast: impact of land use and climate PhD thesis, Monographs of the Boreal Environment Research. Vol. 36.

Mattsson, T., Kortelainen, P., Laubel, A., Evans, D., Pujo-Pay, M., Räike, A., Conan, P., 2009. Export of dissolved organic matter in relation to land use along the European climatic gradient. Sci. Total Environ 40, 1967–1976.

Mattsson, T., Kortelainen, P., Räike, A., 2005. Export of DOM from boreal catchments: impacts of land use cover and climate. Biogeochemistry 76, 373–394.

Osburn, C.L., Stedmon, C.A., 2011. Linking the chemical and optical properties of dissolved organic matter in the Baltic-North Sea transition zone to differentiate three allochthonous inputs. Mar. Chem 126, 281–294.

Ostapenia, A.P., Parparov, A., Berman, T., 2009. Lability of organic carbon in lakes of different trophic status. Freshw. Biol 54, 1312–1323.

Pitkänen, H., Tamminen, T., 1995. Nitrogen and phosphorus as production limiting factors in the estuarine waters of the eastern Gulf of Finland. Mar. Ecol. Prog. Ser 129, 283–294.

Pitkänen, H., Lehtoranta, J., Peltonen, H., 2008. The Gulf of Finland. In: Schiewer, U. (Ed.), Ecology of Baltic Coastal Waters. Springer-Verlag, Berlin.

Quilbé, R., Rousseau, A.N., Duchemin, M., Poulin, A., Gangbazo, G., Villeneuve, J.-P., 2006. Selecting a calculation method to estimate sediment and nutrient loads in streams: application to the Beaurivage River (Québec, Canada). J. Hydrol 326, 295–310.

Räike, A., Kortelainen, P., Mattsson, T., Thomas, D.N., 2012. 36 year trends in dissolved organic carbon export from Finnish rivers to the Baltic Sea. Sci. Total Environ 435–436, 188–201.

Schlitzer, R., 2014. Ocean Data View. http://odv.awi.de.

Seitzinger, S.B., Sanders, R.W., Styles, R., 2002. Bioavailability of DON from natural and anthropogenic sources to estuarine plankton. Limnol. Oceanogr 47 (2), 353–366.

Seppälä, J., Ylöstalo, P., Kaitala, S., Hällfors, S., Raateoja, M., Maunula, P., 2007. Ship-of-opportunity based phycocyanin fluorescence monitoring of the filamentous cyanobacteria bloom dynamics in the Baltic Sea. Estuar. Coast. Shelf Sci 73, 489–500. http://dx.doi.org/10.1016/j.ecss.2007.02.015.

Solórzano, L., 1969. Determination of ammonia in natural waters by the phenolhypochlorite method. Limnol. Oceanogr 14 (5), 799–801.

Spilling, K., Ylöstalo, P., Simis, S., Seppälä, J., 2015. Interaction effects of light, temperature and nutrient limitations (N, P and Si) on growth, stoichiometry and photosynthetic parameters of the cold-water diatom *Chaetoceros wighamii*. PLoS One 10 (5), e0126308. http://dx.doi.org/10.1371/journal.pone.0126308.

Stålnacke, P., Grimvall, A., Sundbland, K., Tonderski, A., 1999. Estimation of riverine loads of nitrogen and phosphorus to the Baltic Sea, 1970–1993. Environ. Monit. Assess 58, 173–200.

Stålnacke, P., Pengerud, A., Vassiljev, A., Smedberg, E., Mörth, C.-M., Hägg, H.E., Humborg, C., Andersen, H.E., 2015. Nitrogen surface water retention in the Baltic Sea drainage basin. Hydrol. Earth Syst. Sci 19, 981–996.

Stedmon, C.A., Osburn, C.L., Kragh, T., 2010. Tracing water mass mixing in the Baltic–North Sea transition zone using the optical properties of coloured dissolved organic matter. Estuar. Coast. Shelf Sci 87, 156–162.

Stedmon, C.A., Markager, S., 2003. Behaviour of the Optical Properties of Coloured Dissolved Organic Matter under Conservative Mixing. Estuar. Coast. Shelf Sci 57. http://dx.doi.org/10.1016/S0272-7714(03)00003-9.

Stedmon, C.A., Nelson, N.B., 2015. The Optical Properties of DOM in the Ocean. In: Hansell, D.A., Carlson, C.A. (Eds.), Biogeochemistry of Marine Dissolved Organic Matter, second ed. Elsevier, pp. 481–508.

Stedmon, C.A., Markager, S., Kaas, H., 2000. Optical properties and signatures of chromophoric dissolved organic matter (CDOM) in Danish coastal waters. Estuar. Coast. Shelf Sci 51, 267–278.

Stedmon, C.A., Markager, S., Tranvik, L., Kronberg, L., Slätis, T., Martinsen, W., 2007. Photochemical production of ammonium and transformation of dissolved organic matter in the Baltic Sea. Mar. Chem 104, 227–240.

Stepanauskas, R., Jørgensen, N.O.G., Eigaard, O.R., Žvikas, A., Tranvik, L.J., Leonardson, L., 2002. Summer inputs of riverine nutrients to the Baltic Sea: bioavailability and eutrophication relevance. Ecological Monograms 74, 579–597.

Tamminen, T., Andersen, T., 2007. Seasonal phytoplankton nutrient limitation patterns as revealed by bioassays over Baltic Sea gradients of salinity and eutrophication. Mar. Ecol. Prog. Ser 340, 121–138.

Thomas, H., Pempkowiak, J., Wulff, F., Nagel, K., 2010. The Baltic Sea. In: Liu, K.-K., Atkinson, L., Quinones, R.A., Talaue-McManus, L. (Eds.), Carbon and Nutrient Fluxes in Continental Margins. Springer-Verlag, Berlin.

Thrane, J.-E., Hessen, D.O., Andersen, T., 2014. The absorption of light in lakes: negative impact of dissolved organic carbon on primary productivity. Ecosystems http://dx.doi.org/10.1007/s10021-014-9776-2.

UNECE, 2011. Second Assessment of Transboundary Rivers, Lakes and Groundwaters. United Nations, Geneva, p. 428.

Urtizberea, A., Dupont, N., Rosland, R., Aksnes, D.L., 2013. Sensitivity of euphotic zone properties to CDOM variations in marine ecosystem models. Ecol. Model. 256, 16–22.

Vähätalo, A.V., Zepp, R.G., 2005. Photochemical mineralization of dissolved organic nitrogen to ammonium in the Baltic Sea. Environ. Sci. Technol 39, 6985–6992.

von Wachenfeldt, E., Tranvik, L.J., 2008. Sedimentation in boreal lakes—the role of flocculation of allochthonous dissolved organic matter in the water column. Ecosystems 11, 803–814.

Warnock, R.E., Gieskes, W.W.C., van Laar, S., 1999. Regional and seasonal differences in light absorption by yellow substance in the southern Bight of the North Sea. J. Sea Res 42, 169–178.

Wiegner, T.N., Seitzinger, S.P., Glibert, P.M., Bronk, D.A., 2006. Bioavailability of dissolved organic nitrogen and carbon from nine rivers in the eastern United States. Aquat. Microb. Ecol 43, 277–287.

Xie, H., Bélanger, S., Song, G., Benner, R., Taalba, A., Blais, M., Tremblay, J.-É., Babin, M., 2012. Photoproduction of ammonium in the southeastern Beaufort Sea and its biogeochemical implications. Biogeosciences 9, 3047–3061. http://dx.doi.org/10.5194/bg-9-3047-2012.

Yamashita, Y., Nosaka, Y., Suzuki, K., Ogawa, H., Takahashi, K., Saito, H., 2013. Photobleaching as a factor controlling spectral characteristics of chromophoric dissolved organic matter in open ocean. Biogeosciences 10, 7207–7217. http://dx.doi.org/10.5194/bg-10-7207-2013.

Ylöstalo, P., Kallio, K., Seppälä, J., 2014. Absorption properties of in-water constituents and their variation among various lake types in the boreal region. Remote Sens. Environ 148, 190–205.